

ON CFD INVESTIGATION OF RADIAL CLEARANCE OF LABYRINTH SEALS OF A TURBINE ENGINE

MICHAL ČÍZEK^{a,*}, ZDENĚK PÁTEK^b

^a Czech Technical University in Prague, Center of Aviation and Space Research, Jugoslávských partyzánů 1580/3, 16000 Praha, Czech Republic

^b VZLÚ, Czech Aerospace Research Centre, Beranových 130, 19905 Praha, Czech Republic

* corresponding author: michal.cizek@fs.cvut.cz

ABSTRACT. Fluid flow in labyrinth seals of a turbine engine is described. The aim is to describe numerical calculations of fluid flow in labyrinth seals and evaluate the calculated data for different settings of radial clearance of labyrinth seals. The results are achieved by 3D CFD detailed simulations in a typical seal geometry. The calculations are performed for different radial clearances at a constant pressure drop. The calculated data are evaluated based on mass flow, static pressure, total enthalpy and total temperature of air. Based on the calculated data, it is visible that the total temperature of air is increased in the labyrinth seals. The static pressure of air acts as expected – the static pressure is decreased in all teeth. The Mach number is similar in all teeth, but the maximum value is in the last tooth, because of the expansion into the ambient conditions. Results of the calculations are that the total temperature in labyrinth seals is not constant as it is usually presented or supposed in common literature.

KEYWORDS: Labyrinth seal, CFD calculation, turbine engine.

1. INTRODUCTION

This article describes and analyses the flow in a labyrinth seal of a small turbine engine. The objective is to analyse the air flow for a constant pressure drop in the seals with different geometrical settings – it means different radial clearances between rotor and stator and different numbers of teeth. Generally, the labyrinth seals work in a turbine engine to prevent the air flow enter the engine modules, where the flow is useless, because the turbine disc is screwed to the shaft – it is a rotating part. The air flow is primarily used to cool turbine blades, turbine discs, shafts etc. (see [1]). Thanks to the labyrinth seals, it is possible to direct the air flow to the parts of the engine where it can be useful – which means decrease the axial force of the shaft, etc. (see [2]). In numerical analysis, it is important to correctly design and define the cavity between the rotating and non-rotating parts, because the tooth profile has an important influence at high Mach numbers (see [1, 3]). Historically, the research of the labyrinth seals has been executed more extensively on steam turbines than on aircraft turbine engines (see [1, 4]). The steam turbines use the labyrinth seals specially to reduce the mass flow over the top of turbine blades and to increase the efficiency of the turbine [4]. In steam turbines, the radial clearance has a higher influence on the turbine performance than in the turbine engine. But when the radial clearance is too large in a critical part of the turbine engine, the influence on the engine performance parameters (e.g. fuel consumption) is more pronounced than with the standard clearance (see [5]).

This is because the turbine has bigger dimensions than the engine (see [1, 4, 6]). In a small aviation turbine engine, the device continually changing the radial clearance during the flight cannot be used. It is not technically a problem, but there is a problem with weight. This is the reason why it is necessary to understand the airflow in cavities between the rotating and non – rotating parts (see [7, 8]). The way to understanding the flow is through the CFD simulation (see [9]). The setup of the simulation is that the part with teeth rotates – as resulted from [10], where only the rotor wall rotated. The stator parts are located in front of and after the rotor part. The future evaluation of the calculations will be performed by the measurements of the rotating part of labyrinth teeth (see [11, 12]). Thermodynamically, the process in the labyrinth seal is a conversion of kinetic energy of the shaft to the heat energy of the flow (see [1]). The thermal energy manifests itself by a higher total temperature and a higher enthalpy of air flow. Generally, the dissipation of the kinetic energy is important factor, but typically, dimensions of a small turbine engine render it relatively negligible. It is very difficult situation for engine designers.

The aim of this work is directly defined: clarify why the temperature is increased. The way of clarification of the problem is a thorough detailed numerical analysis of this problem. The analysis is based on the CFD calculation of labyrinth seals of the turbine engine. At the end, the engine designer would have more information about the temperature through the labyrinth seal. Designer will be able to better define

Hub Radius	86.5	mm
Tip Radius	89	mm
Length of Rotor Part	17	mm
Length of Stator Part	21	mm

TABLE 1. Geometrical parameters.

the material of the seal with respect to the conditions of its use.

2. GEOMETRICAL DESCRIPTION

The labyrinth seals of a small turbine engine in the CFD calculation are composed of rotor and stator parts. The stator part is formed by a non-rotational surface (see Fig. 1). The rotor part consists of a shaft with teeth. The shaft is rotating with a predetermined constant speed (see Fig. 2). The swirl is on surfaces between the selected teeth - there are two surfaces between the teeth where the swirl is created. Thanks to the circumferential swirl, the kinetic energy of the air flow (the similar geometry is in [7]) is thwarted (details of the geometrical parameters are in Tab. 1). The geometric parameters correspond to the small turbine engine.

The rotor of the labyrinth seals consists of straight teeth that are tapered on the external side. There is a thin slab on the spike, which is left behind due to technological reasons (see Fig. 3). For a better quality of the air flow, the tooth should be as sharp as possible. In an ideal situation, it should be a sharp edge. This geometry is a compromise between the ideal and real teeth.

3. 3D MODEL AND CALCULATING MESH

Calculating the 3D model for the CFD calculation consists of three basic volumes:

- Inlet control volume – non-rotating
- Sealing volume – rotating (the volume is rotating, but a boundary condition “Counter rotating wall” is set on the wall of the stator - i.e. the face rotates in a reverse direction to the volume – resulting in a stator. This solution was chosen based on the manual [13] and on the discussion with ANSYS CFD specialist)
- Outlet control volume – non-rotating

All three parts are designed as circular cuts with a 5° opening angle. All parts were designed in ANSYS Design Modeler v18. The mesh of the sealing volume is presented in Fig. 4.

The calculating mesh was prepared in ANSYS Meshing v18 software. The inflation function was used on all edges for a better description of fluid flow. Even though the dimensions of the sealing are very small, the inflation on edges is additionally created. In the smallest point of labyrinth seals - the radial clearance between the teeth and stator part – there are 14 rows

of a hexahedral mesh. Created 2.47 mil cells are generated in this settings where 5 teeth are used in the sealing volume. In the inlet and outlet control volume, 158 thousand cells are created. “Frozen-Rotor” interfaces are between the rotor and stator parts.

4. BOUNDARY CONDITIONS

All variants were calculated with a constant pressure drop. The total pressure and the total temperature are defined in the inlet control volume. In the outlet control volume, static pressure is defined (see Tab. 2). Rotating sealing volume is defined by a constant rotating speed. Rotating speed means that the sealing volume rotates at a constant speed. Air ideal gas is used as the fluid of flow. The fluid model of heat transfer is Total Energy and the turbulence model defined by $k - \varepsilon$. The boundaries of the volumes are defined by periodic conditions to save the calculating time (see Fig. 5). ANSYS CFX v18 software was used for the calculations.

The $k - \varepsilon$ model was selected based on a preliminary analysis of the turbulent models. There were three turbulent models tested at a constant radial clearance, the identical mesh and the identical boundary conditions:

- $k - \varepsilon$
- SST (Shear Stress Transport)
- RNG $k - \varepsilon$

The analysis was performed using total temperature and mass flow differences in the first and the last teeth of the labyrinth seal. Results of this preliminary analysis show that $k - \varepsilon$ is the best turbulent model (see Fig. 7 and Fig. 6). The $k - \varepsilon$ turbulent model shows good results with a reasonable computing time. It also has a wall function for a better description of the boundary layer. Similar results can be found in [2] and [9].

5. RESULTS OF THE CALCULATION

The calculation model was finished in 1000 iterations (see Fig. 8 and Fig. 9, where a convergence of residuals and of the mass flow through the labyrinth seals is visible).

Time steps are different for a specific number of iterations (see Tab. 3).

The calculated thermodynamic parameters are evaluated by the following formulas:

- Mass flow is represented by dimensionless flow coefficient:

$$Q_{CORR} = \frac{Q}{Q_{REF}} \quad (1)$$

- Static pressure is represented by dimensionless pressure coefficient:

$$p_{SCORR} = \frac{p_S}{p_{SREF}} \quad (2)$$

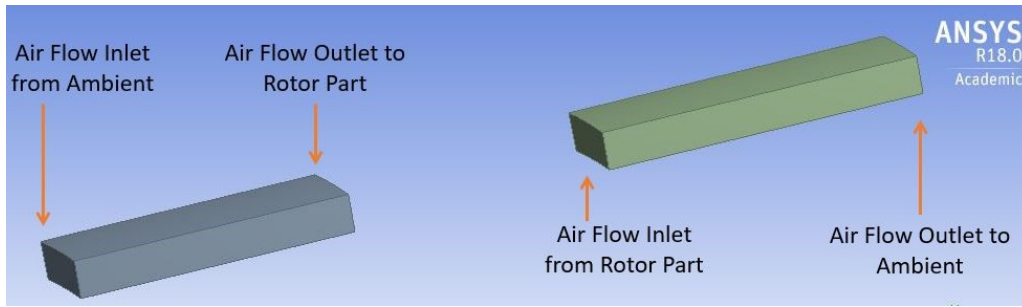


FIGURE 1. Stator parts.

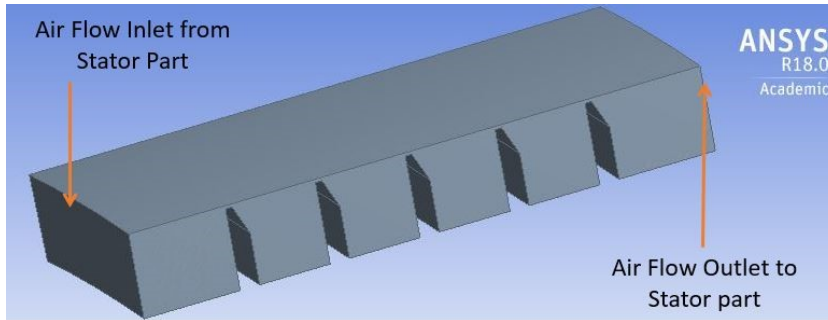


FIGURE 2. Rotor part.

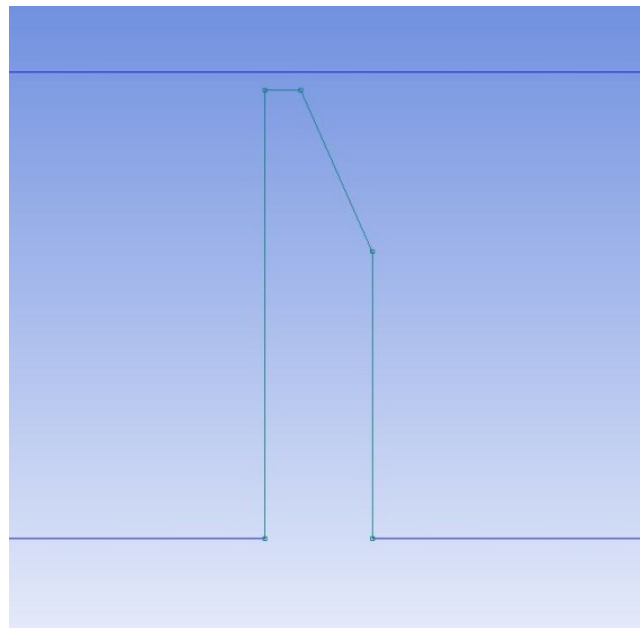


FIGURE 3. Teeth.

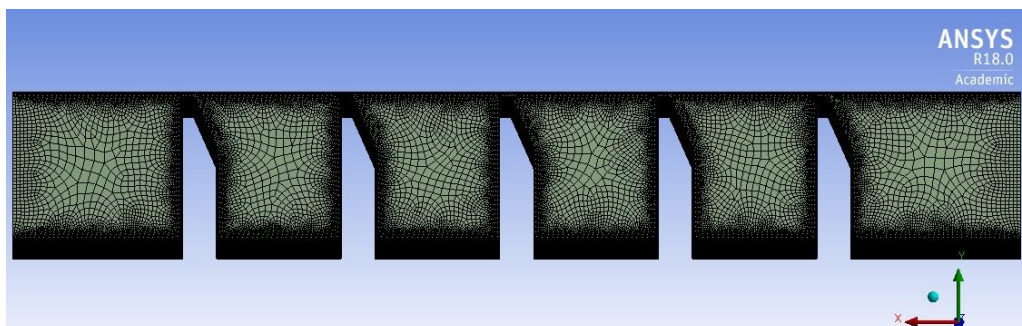


FIGURE 4. Mesh of labyrinth seals.

Pressure ratio [kPa]	Inlet total temperature [K]	Inlet total pressure [kPa]	Rotating speed [RPM]
1.3	542	660	35e+03

TABLE 2. Boundary conditions.

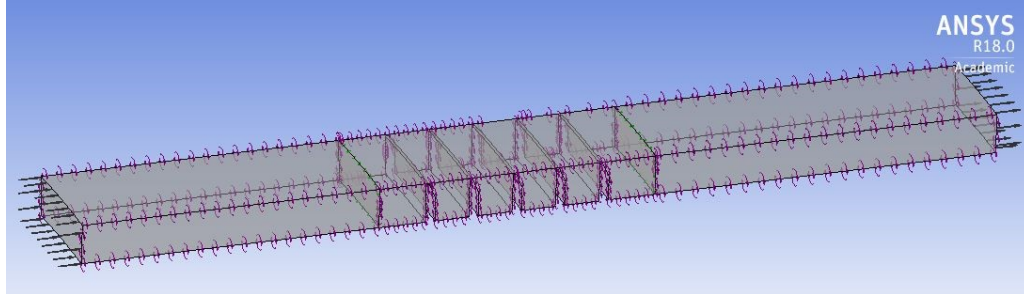


FIGURE 5. Boundary and periodic conditions.

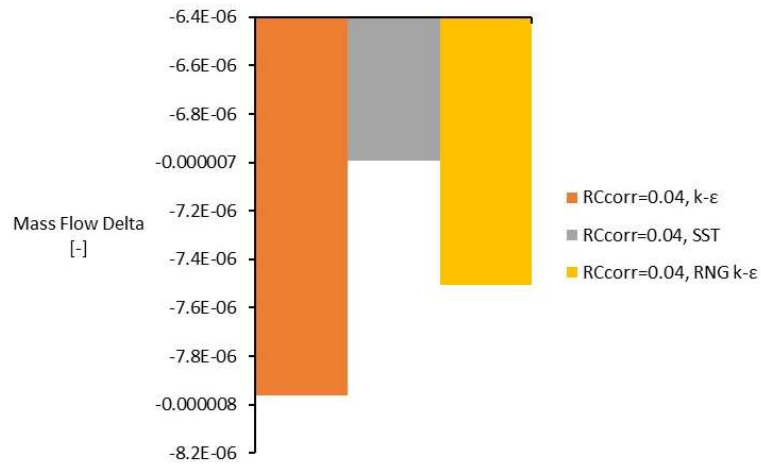


FIGURE 6. Turbulent model comparison.

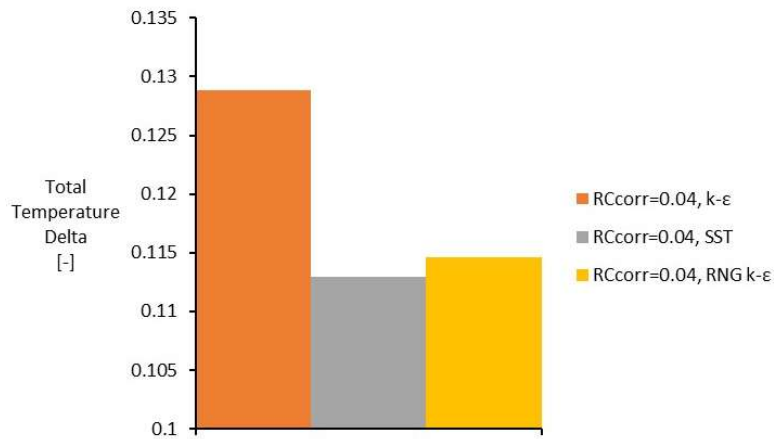


FIGURE 7. Turbulent model comparison.

Number of iterations	Time step [s]
1	10E-6
300	10E-5
500	10E-4
1000	10E-4

TABLE 3. Time steps.

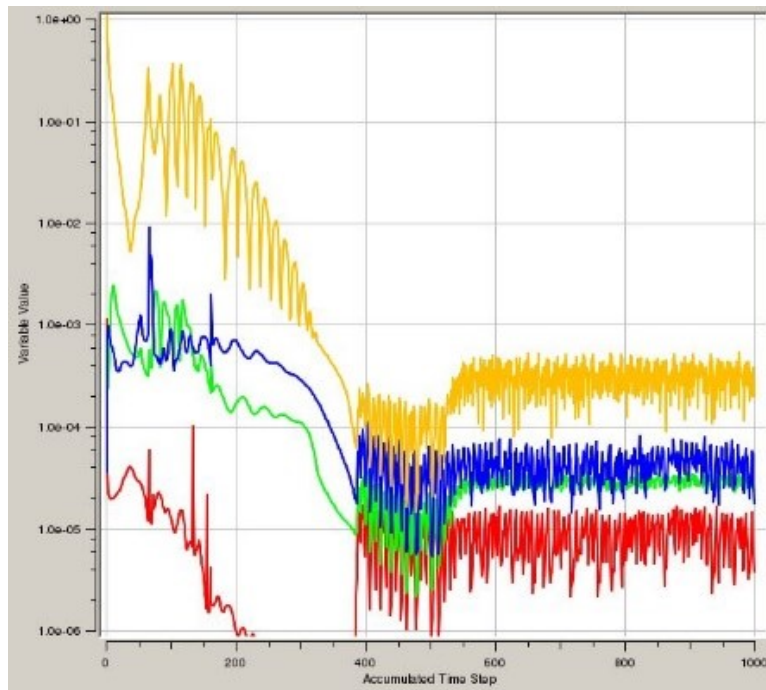


FIGURE 8. Convergence of residuals.

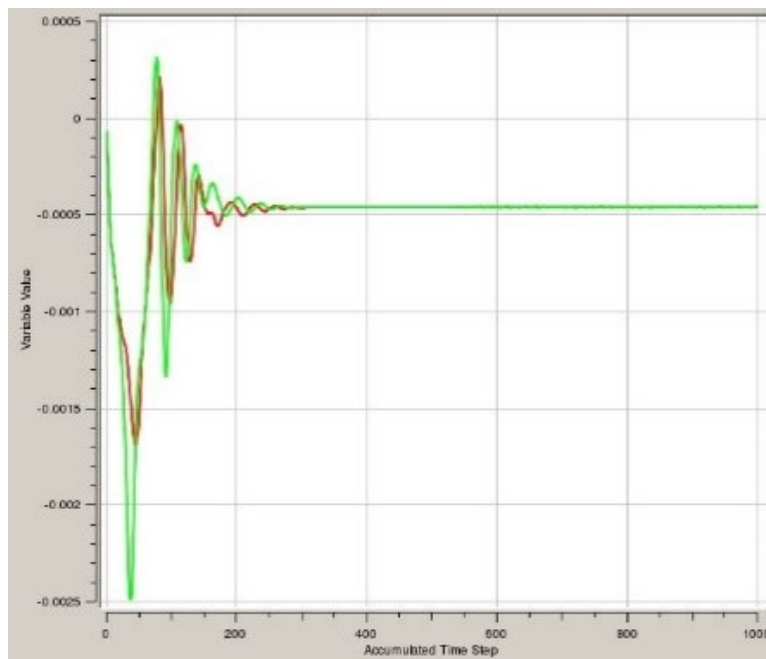


FIGURE 9. Convergence of mass flow.

- Total temperature is represented by dimensionless temperature coefficient:

$$T_{CCORR} = \frac{T_C}{T_{CREF}} \quad (3)$$

- Total enthalpy is represented by dimensionless enthalpy coefficient:

$$h_{CORR} = \frac{h}{h_{REF}} \quad (4)$$

- The radial clearance is represented by dimensionless clearance:

$$RC_{CORR} = \frac{RC}{RC_{REF}} \quad (5)$$

The reference values of thermodynamic parameters were established by the ambient conditions corresponding to a standard operation of the turbine engine. The reference value of the radial clearance is the height of the flow channel without the teeth (see Tab. 4).

The field of Mach number through all 5 teeth and $RCCORR$ from 0.02 to 0.06 are presented in pictures from Fig. 10 to Fig. 12. The highest Mach number is in the last teeth. In chambers between the teeth, lower speeds than in the radial clearance area can be observed.

In the following charts, calculations with a constant number of teeth and variable radial clearance are presented. In charts from Fig. 18 to Fig. 19, the standard thermodynamic parameters that were calculated by the CFD calculation are presented. In X-axis, the number of teeth is shown. It is possible to see the trend of the thermodynamic parameters in all teeth (not only inlet and outlet). Due to this fact, it should be possible to better understand which thermodynamic phenomena are in the teeth. In Y-axis, the thermodynamic parameters (by dimensionless values) that are present in (1) to (5) formulas are shown. In charts, 3 lines represent 3 different radial clearances.

In the following figures (from Fig. 13 to Fig. 15), the velocity vectors in the labyrinth seals are presented.

The decreasing mass flow (seen in Fig. 17) is explained as a numerical error. Based on the convergence analysis of the mass flow that is presented in Fig. 9, it is seen that the inlet and outlet mass flows are identical. After all, the values in Fig. 17 are very small.

6. RESULTS AND DISCUSSION

In the previous paragraph, the steps of the CFD calculation in the labyrinth seals were summarized. The geometrical setting is different in comparison with the original geometrical setting in [10]. The original idea was without the non-rotating parts. Regarding the parts with teeth, only the wall with teeth was rotating. Based on results of the analysis, it was decided that the simulation is not so accurate. The fluid model was modified to achieve a better description – inlet and outlet non-rotating parts and rotating

parts with teeth. The calculation mesh that is presented in Fig. 4 is equivalent to the calculating mesh in [7, 14, 15]. Based on this analysis, the mesh is usable and fully and properly functioning.

The Mach number field through the teeth corresponds to the expectations based on thermodynamics (see Fig. 10, Fig. 11 and Fig. 12). From the flow field, it can be seen that the maximum speed is in the last tooth, which has the greatest effect on the flow in labyrinth seals. The maximum Mach number is in the position of a maximal radial clearance. From the velocity vectors field (see Fig. 13, Fig. 14 and Fig. 15), similar results like from Mach number field can be seen, and the velocity vortexes are fully developed in cells between the teeth. The trends of a non-dimensional static pressure (see Fig. 16) and mass flow (see Fig. 17) are as expected, because the trends are decreasing. This assumption can be observed by decreasing static pressure and decreasing mass flow at a constant pressure drop. These trends are visible in all situations with a different radial clearance. Fig. 17 shows that the minimum mass flow through the seals is reached when the minimum radial clearance (orange line) was used. Different situation is in the trend of non-dimensional total temperature (see Fig. 18) and total enthalpy (see Fig. 19). With the minimum radial clearance (orange line), the temperature gradient reaches its maximum ($\Delta T_{CCORR} \cong 0.26$). With the maximum radial clearance (green line), the temperature gradient reaches its minimum ($\Delta T_{CCORR} \cong 0.12$). The identical trend is observed in enthalpy. The maximum enthalpy gradient is reached with the minimum radial clearance ($\Delta h_{CORR} \cong 0.29$) and the minimum enthalpy gradient is reached with the maximum radial clearance ($\Delta h_{CORR} \cong 0.14$).

Regarding the velocity distribution in [2, 15] with velocity vectors in Fig. 13, Fig. 14 and Fig. 15, the velocity vectors are similar. The rotating swirl is fully developed - the labyrinth seal is working correctly, as it can be seen when comparing the pressure distribution in [7] and static pressure distribution in Fig. 16, where the pressure is decreased. This corresponds with the labyrinth seal theory [1]. The mass flow through the labyrinth seals in Fig. 17 is similar as the one in [3]. The Mach number distribution in Fig. 10, Fig. 11 and Fig. 12 is comparable with results in [7]. The Mach number distribution is logic – maximum Mach number is in the last tooth because of the expansion to the ambient conditions.

Based on the above-mentioned facts, it can be stated that the labyrinth seal calculation is correct in the sense that it provides results corresponding to basic thermodynamic considerations. The result of the total temperature distribution is that the total temperature is not constant in all teeth. The values of static pressure and mass flow distribution is decreasing in all teeth. The values of total enthalpy distribution is increasing in all teeth.

p_{SREF} [kPa]	T_{CREF} [K]	h_{REF} [kJ·kg ⁻¹]	Q_{REF} [kg·s ⁻¹]	RC_{REF} [mm]
101	288	260	0.01	2.5

TABLE 4. Reference conditions.

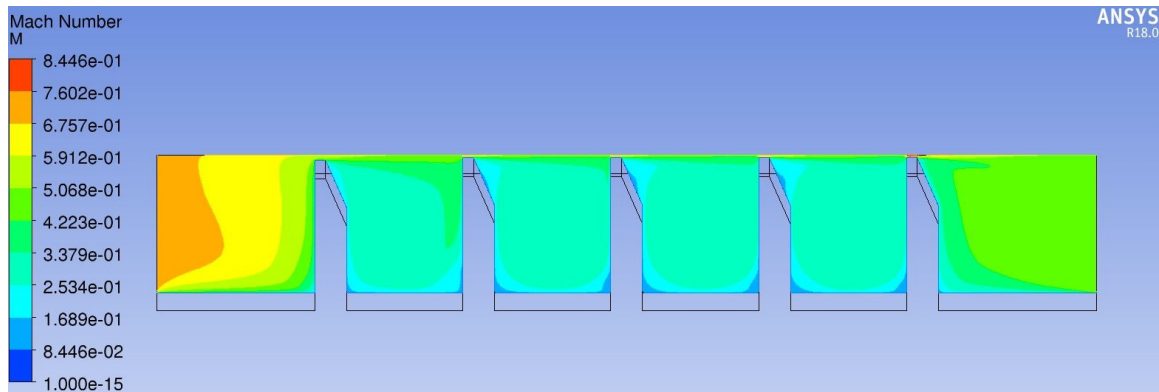


FIGURE 10. Mach number field – $RC_{CORR} = 0.02$.

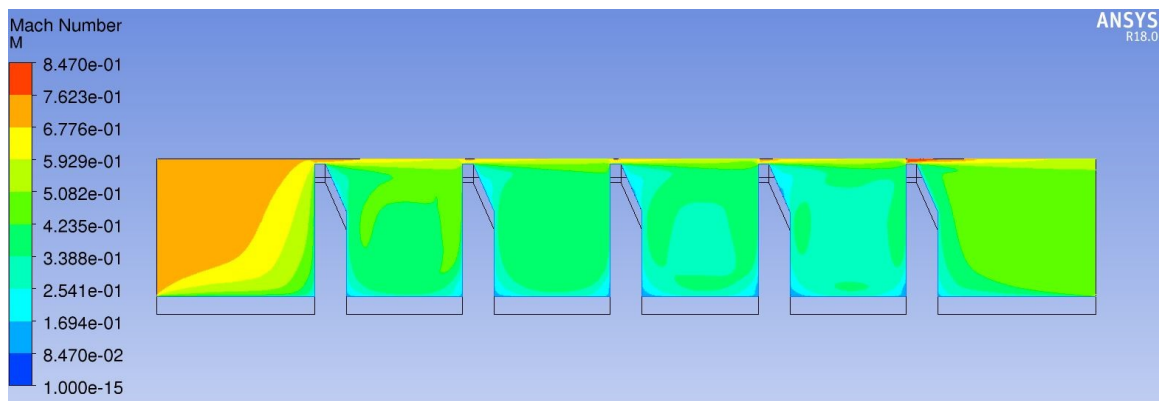


FIGURE 11. Mach number field – $RC_{CORR} = 0.04$.

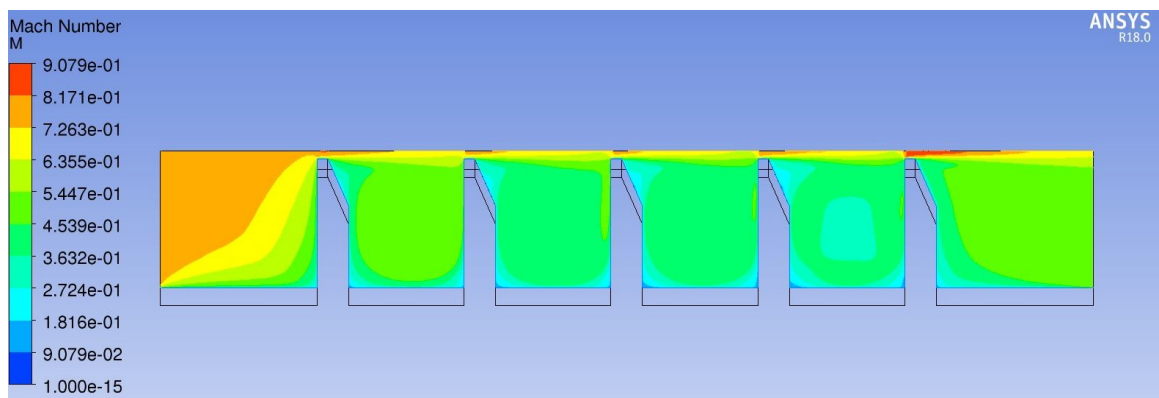


FIGURE 12. Mach number field – $RC_{CORR} = 0.06$.

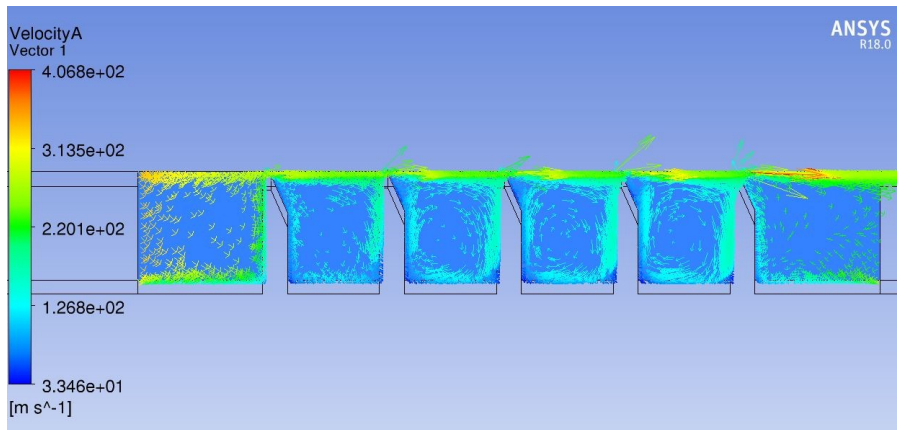


FIGURE 13. Velocity vectors – $RC_{CORR} = 0.02$.

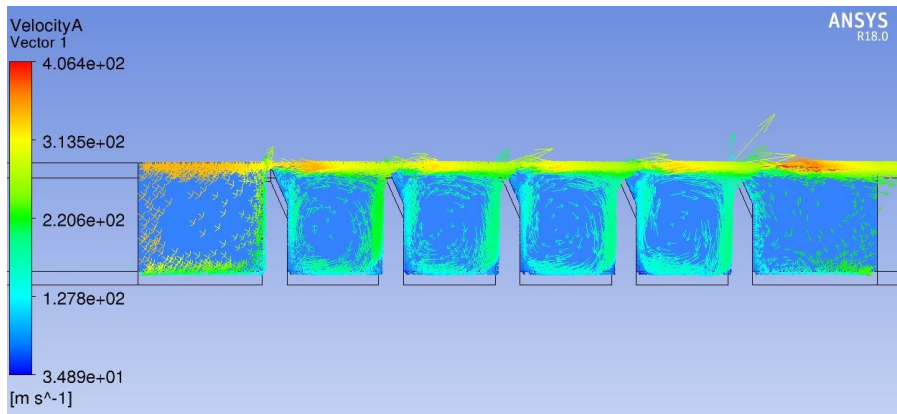


FIGURE 14. Velocity vectors – $RC_{CORR} = 0.04$.

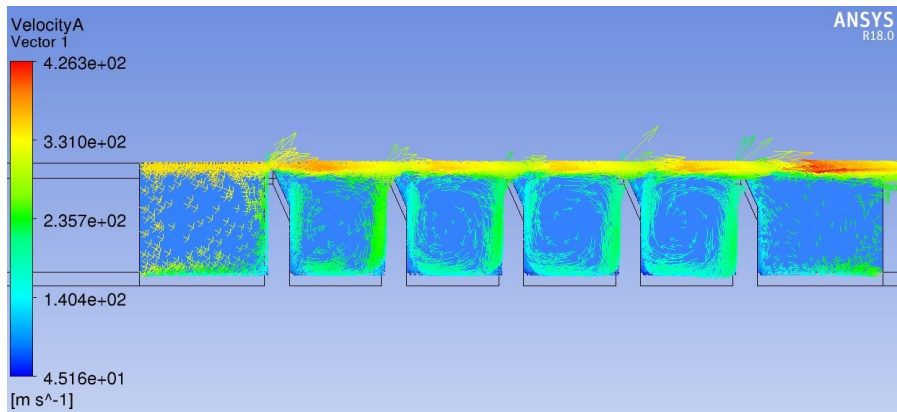


FIGURE 15. Velocity vectors – $RC_{CORR} = 0.06$.

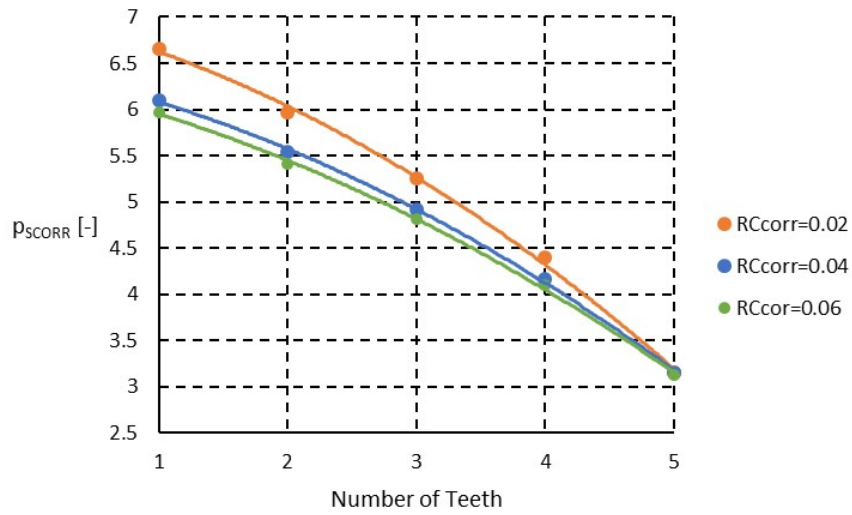


FIGURE 16. Non-dimensional static pressure.

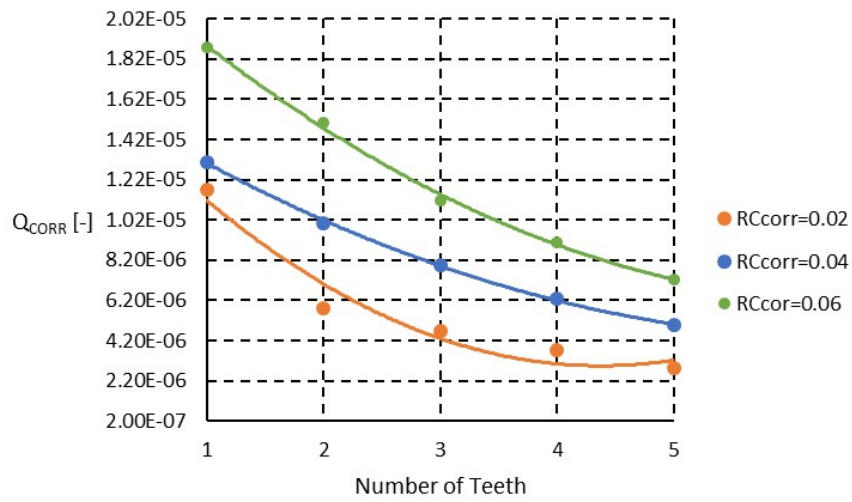


FIGURE 17. Non-dimensional mass flow.

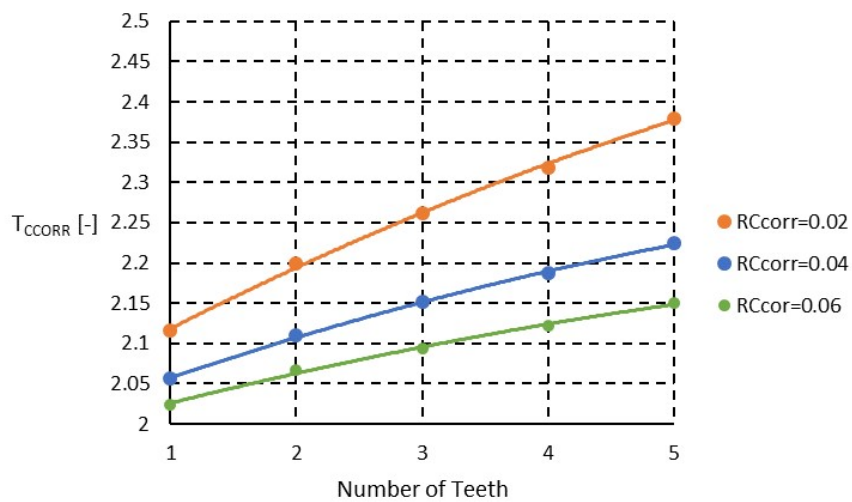


FIGURE 18. Non-dimensional total temperature.

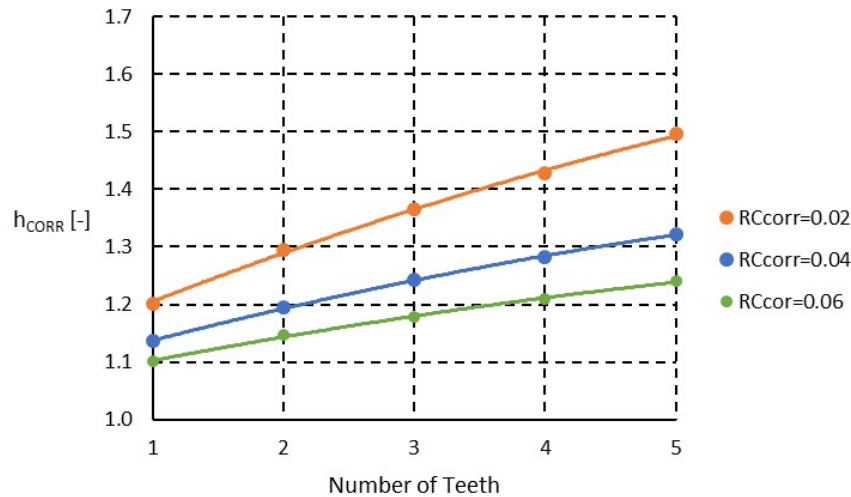


FIGURE 19. Non-dimensional total enthalpy.

7. CONCLUSIONS

The conclusions from the calculations consider the fact that the total temperature and enthalpy are increasing, because of the shaft kinetic energy conversion to the heat energy, which disproved the frequently used assumption that the temperature is constant. This new knowledge can be important for the design of aircraft turbine engines. The designers can improve the design of the shaft of the turbine and thus improve the performance characteristics of the engine. When the temperature gradients in all teeth are calculated more precisely, the appropriate material of the shaft can be chosen accordingly. Based on it, harmful vibrations of the shaft that are dangerous for the engine (see [1]) can be eliminated.

As the next step, these studies should be carried out:

- (1.) The loss performance parameter (e.g. power) should be analysed.
- (2.) The development of enthalpy and total temperature and static pressure should be experimentally tested.

After the loss performance parameter analysis in teeth (point 1), it should be interesting to analyse the stability of the flow path. This should be important for a better evaluation of the calculated data and also it should be helpful for the design or appropriate selection of an experimental laboratory where the seals should be tested.

After the experimental tests of labyrinth seals, it would be possible to evaluate the calculated data and the CFD model of seals would be modified accordingly. Then, the calculation model could be simplified and modified to be more user friendly.

LIST OF SYMBOLS

RC radial clearance [mm]
 Q mass flow [kg s^{-1}]

p_s static pressure [Pa]

x_2 mixing ratio of eggshells to anthill clay

T_C total temperature [K]

h total enthalpy [J kg^{-1}]

Subscripts

$CORR$ corrected

REF reference

ACKNOWLEDGEMENTS

Authors acknowledge support from the ESIF, EU Operational Programme Research, Development and Education, and from the Center of Advanced Aerospace Technology (CZ.02.1.01/0.0/0.0/16_019/0000826), Faculty of Mechanical Engineering, Czech Technical University in Prague.

REFERENCES

- [1] J. Jerie. *Teorie motorů*. Ediční středisko ČVUT, Prague, 1981.
- [2] G. Ilieva, C. Pirovsky. Labyrinth seals with application to turbomachinery. *Materials Science & Engineering Technology* **50**(5):479 – 491, 2019. DOI:10.1002/mawe.201900004.
- [3] G. Bondarenko, V. Baga, I. Bashlak. Flow simulation in a labyrinth seal. In *Problems of Mechanics in Pump and Compressor Engineering*, vol. 630 of *Applied Mechanics and Materials*, pp. 234 – 239. Trans Tech Publications Ltd, 2014. DOI:10.4028/www.scientific.net/AMM.630.234.
- [4] A. V. Ščeglajev. *Parní turbíny 1*. Nakladatelství technické literatury, Prague, 1983.
- [5] H. L. Stocker. Advanced Labyrinth Seal Design Performance for High Pressure Ratio Gas Turbines. In *ASME 1975 Winter Annual Meeting: GT Papers*, vol. Turbo Expo: Power for Land, Sea, and Air. 1975. DOI:10.1115/75-WA/GT-22.
- [6] J. A. Demko. *The Prediction and Measurement of Incompressible Flow in a Labyrinth Seal*. Ph.D. thesis, Texas A&M University, 1986.

- [7] J. Fürst. Numerical simulation of flows through labyrinth seals. In *Engineering Mechanics 2015*, vol. 821 of *Applied Mechanics and Materials*, pp. 16 – 22. 2016. DOI:10.4028/www.scientific.net/AMM.821.16.
- [8] H. Zimmermann. Some Aerodynamic Aspects of Engine Secondary Air Systems. In *Turbo Expo: Power for Land, Sea, and Air*, vol. 1: Turbomachinery. 1989. DOI:10.1115/89-GT-209.
- [9] L. San Andrés, T. Wu. Leakage and Dynamic Force Coefficients for Two Labyrinth Gas Seals: Teeth-on-Stator and Interlocking Teeth Configurations — A CFD Approach to Their Performance. In *Turbo Expo: Power for Land, Sea, and Air*, vol. 7B: Structures and Dynamics. 2018. DOI:10.1115/GT2018-75205.
- [10] M. Čížek. Chambers of Labyrinth Seals of Turbine Engine. In *New Trends of Civil Aviation 2018, Conference proceedings*. 2018.
- [11] D. Sun, S. Wang, C.-W. Fei, et al. Numerical and experimental investigation on the effect of swirl brakes on the labyrinth seals. *Journal of Engineering for Gas Turbines and Power* **138**(3), 2015. DOI:10.1115/1.4031562.
- [12] H. L. Chae. *A Numerical and Experimental Study of Windback Seals*. Ph.D. thesis, Texas A&M University, 2009.
- [13] ANSYS Help Viewer 18.0, 2016.
- [14] J. J. Moore. Three-Dimensional CFD Rotordynamic Analysis of Gas Labyrinth Seals. *Journal of Vibration and Acoustics* **125**(4):427 – 433, 2003. DOI:10.1115/1.1615248.
- [15] T. Wu, L. S. Andrés. Gas labyrinth seals: On the effect of clearance and operating conditions on wall friction factors – A CFD investigation. *Tribology International* **131**:363 – 376, 2019. DOI:10.1016/j.triboint.2018.10.046.